electronic materials

Article

Tunnel Spin-Polarization of Ferromagnetic Metals and Ferrimagnetic Oxides and Its Effect on Tunnel Magnetoresistance

Gunnar Suchaneck

Solid-State Electronics Laboratory, TU Dresden, 01062 Dresden, Germany; gunnar.suchaneck@tu-dresden.de

Abstract: This work presents an examination and unification of fragmented data on spin polarization in half-metallic, ferrimagnetic oxides. It also includes well understood ferromagnetic metals for comparison. The temperature and disorder dependencies of the spin polarization are evaluated. Both the temperature dependence of the tunnel magnetoresistance and, for the very first time, its temperature coefficient are calculated based on the simplified Julliére model. The tunnel magnetoresistance in the magnetic tunnel junctions deteriorates due to the temperature dependence of the spin polarization the lower the Curie temperature is. As a result, magnetic tunnel junctions—consisting of ferromagnetic oxides with a Curie temperature not far above room temperature—are not promising for room temperature applications. Additionally, ferrimagnetic oxides possessing a Curie temperature below 650 K are not suitable for room temperature applications because of an unacceptable temperature coefficient exceeding −2%.

Keywords: spintronics; tunneling magnetoresistance; spin-polarization; temperature coefficient

check for updates

Citation: Suchaneck, G. Tunnel Spin-Polarization of Ferromagnetic Metals and Ferrimagnetic Oxides and Its Effect on Tunnel Magnetoresistance. *Electron. Mater.* **2022**, *3*, 227–234. https://doi.org/10.3390/electronicmat3030019

Academic Editor: Wojciech Pisula

Received: 22 June 2022
Accepted: 25 July 2022
Published: 28 July 2022

1. Introduction

Spintronics (spin-transport electronics) was born in 1988 as a result of the discovery of giant magnetoresistance (GMR) in Fe/Cr multilayer structures [1,2], honored by the 2007 Nobel Prize in physics. Within 10 years, GMR read heads in hard disks were introduced into the market as first-generation spintronic devices and revolutionized the magnetic mass storage industry. Later, GMR was superseded in most applications by devices based on the tunnel magnetoresistance (TMR) [3]. Both the GMR-based and TMR-based devices consist of thin-film structures, including two ferro(ferri)magneic (FM) layers with a nonmagnetic interlayer. Similar to GMR, the resistance of the TMR junction is linked to the relative orientation of the magnetization of the two FM electrodes.

Nowadays, spintronics continues its development via the investigation of a wide variety of spin-dependent transport and transfer processes, novel materials, phenomena, and device concepts. However, there are still many open questions and challenges [4].

Spin-dependent tunneling was first investigated in a Ni/Al thin-film structure, where the density of states in superconducting Al splits in a high magnetic field into spin-up and spin-down-states forming a gap [5]. The TMR was obtained in 1975 in thin-film stacks with insulating tunneling barriers placed between two FM layers [6]. It was shown that the TMR effect originated in spin-dependent tunneling. In 1995, improved technologies allowed for the fabrication of magnetic tunnel junctions (MTJs) that showed resistance changes that were interesting for applications, e.g., at room temperature [7,8]. Later, it turned out that TMR can significantly exceed GMR in terms of resistance change [9–12]. It has to be noted that the high TMR in MTJs possessing a MgO barrier was attributed to a coherent tunneling effect [9].

According to the simplified Julliére model [6], a near 100% spin polarization is a prerequisite for a huge TMR. Another pertinent parameter for spin-dependent tunneling is not the spin-polarization of the FM surface but that of the FM/tunnel barrier interface since spin polarization determined from tunneling experiments is not an intrinsic property of the

FM electrodes. It depends on the barrier material [13], the barrier height [14], the electronic structure of the barrier [15], and the nature of the counter electrode [16]. The electronic structure affects the spin polarization via the position of the Fermi level with respect to the electronic levels above and below the gap of the insulator [17] and the actual profile of the potential barrier [18]. Other parameters having an impact on spin polarization are the presence of nonmagnetic metal impurities and disorder in the barrier layer [19].

The ideal spin polarization of 100% is realized in ideal half-metals, where electron conduction occurs exclusively by charge carriers of one spin direction. In reality, materials exhibiting a half-metallic character consist of two conduction channels, e.g., in the case of $Sr_2FeMo_{6-\delta}$ (SFMO), a semiconducting one for the up-spin band and a metallic one for the down-spin band. Here, only the latter is continuous at the Fermi level [20].

The aim of this work is an examination and unification of fragmented data on spin polarization in half-metallic, ferrimagnetic oxides. For comparison, well understood ferromagnetic metals are also included. The temperature and disorder dependencies of the spin polarization are evaluated. Based on these results, both the temperature dependence of the tunnel TMR and, for the very first time, its temperature coefficient are estimated based on the simplified Julliére model.

2. Methods

In the simplest model, the TMR is determined by the amount of spin-polarization of the two FM layers P_1 and P_2 as [6]

$$TMR = \frac{2P_1P_2}{1 - P_1P_2}. \tag{1}$$

Within this Jullière model, spin polarization is defined in terms of the density of states for up and down spins, $n_\uparrow(E_F)$ and $n_\downarrow(E_F)$, correspondingly:

$$P = \frac{n_\uparrow(E_F) - n_\downarrow(E_F)}{n_\uparrow(E_F) + n_\downarrow(E_F)}. \tag{2}$$

Since the tunneling matrix element for *s*-electrons is much larger than that of *d*-electrons, which in turn define $n(E_F)$ [21], the tunneling spin polarization is superiorly determined via the spin-up and spin-down current densities [22]:

$$P_T = \frac{J_\uparrow - J_\downarrow}{J_\uparrow + J_\downarrow}, \tag{3}$$

which transforms to [23]

$$P_T = \frac{n_\uparrow(E_F)|T_\uparrow|_2 - n_\downarrow(E_F)|T_\downarrow|^2}{n_\uparrow(E_F)|T_\uparrow|_2 + n_\downarrow(E_F)|T_\downarrow|^2}, \tag{4}$$

where $T_\uparrow$ and $T_\downarrow$ are spin-dependent tunneling matrix elements. These matrix elements are determined by wave function overlap at the interface and should generally differ for the spin-up and spin-down bands. In Equation (1), the spin is supposed to be conserved. The TMR is then governed solely by the spin polarization of each of the FM electrodes. Thus, the Jullière model implies that all one needs to build a proper TMR-device is to find FM electrodes with the highest possible spin polarization at room temperature. In this work, we consider a tunnel spin polarization derived from experimental TMR data by means of Equation (1). This value takes into account the interaction with the dielectric barrier. It will be different from the values determined for single FM layers from spin polarization experiments.

A dynamical theory of spin-polarized low-energy electron diffraction from ferromagnetic surfaces proves that in the case of only single scattering, the polarization is proportional to the surface magnetization [24]. On the other hand, magnetization and spin

polarization were proposed to have a similar temperature dependence [25] based on the fact that spin polarization scales approximately with the magnetic moment of the alloy as its composition is varied [26]. Such proportionality was also found in ferromagnetic glasses $Ni_{40}Fe_{40}B_{20}$ [27]. A theoretical work [28] yields a $T^{3/2}$ dependence of spin polarization assuming that the tunneling barriers are sufficiently disordered (so that memory of the Bloch momentum parallel to the junction plane is lost upon tunneling). Therefore, we suppose following [25] that the spin polarization resembles the magnetization behavior in the low temperature region known as Bloch's $T^{3/2}$ law:

$$P(T) = P_0(1 - g_P T^{3/2}) = P_0(1 - k g_{M,s} T^{3/2}), \quad (5)$$

with T the temperature. Here, g_P is a fitting parameter. It is also sensitive to surface contaminations and depends on interface chemistry [29]. The parameter $g_{M,s}$ describes the Bloch $T^{3/2}$ law of the surface spontaneous magnetization. The value $g_{M,s}$ is generally larger than that of the bulk due to a reduced coordination of surface atoms. In the ideal case of a free surface at low temperatures possessing a spin interaction solely with the nearest neighbor plane, $g_{M,s}$ is twice the bulk value [30], whereas for the ferromagnetic glass $Ni_{40}Fe_{40}B_{20}$ it amounts to three times the bulk value [27]. A nonmagnetic overlayer will reduce this excess. The fit of the coefficient k to lanthanum-strontium manganite ($La_{2/3}Sr_{1/3}MnO_3$, LSMO) thin films yielded values of k = 4.22 for LSMO/$SrTiO_3$, k = 3.51 for LSMO/TiO_2, and k = 1.13 for LSMO/ $LaAlO_3$, respectively, while in the case of a free LSMO surface, it is k = 9.17 [31].

In the following, we will consider double perovskites exhibiting antisite disorder (ASD) on the B-site. We assume that the dependence of spin polarization on the ASD is similar to the dependence of the magnetization on the ASD [32]. In this case, it is given by

$$P(ASD) = P_0(1 - 2ASD). \quad (6)$$

The TMR then yields [33]:

$$TMR = \frac{2P_0^2(1 - g_P T^{3/2})^2}{1 - P_0^2(1 - g_P T^{3/2})^2}. \quad (7)$$

Supposing an ASD of about 10% and P_0 = 0.9 [34], we arrive at TMR values for SFMO of 214% and 11% at 4 K and room temperature, respectively. Taking spin-independent tunneling into account, the attainable TMR yields [35]

$$TMR = \frac{2P_0^2(1 - g_P T^{3/2})^2 - \beta_{SI}(T)}{1 - P_0^2(1 - g_P T^{3/2})^2 + \beta_{SI}(T)}, \quad (8)$$

where $\beta_{SI}(T)$ is both a temperature- and barrier-dependent coefficient to describe the spin-independent tunneling.

3. Results and Discussion

Table 1 compiles the parameters of Equation (5). The low-temperature spin polarization was taken from literature. For the sake of simplicity, the Bloch´s $T^{3/2}$ coefficients g_P were estimated using the Curie temperature T_C

$$g_P \approx T_C^{-3/2}. \quad (9)$$

They are in satisfactory accordance with previous data of 0.1–0.6 $\times 10^{-5}$ for Co/Al_2O_3 [25], 1.9 $\times 10^{-4}$ for LSMO/$SrTiO_3$, 5.1 $\times 10^{-5}$ for LSMO/$LaAlO_3$, 1.58 $\times 10^{-4}$ for LSMO/TiO_2 [31], and 1.9 $\times 10^{-4}$ for SFMO/$SrTiO_3$ [34]. Table 1 also includes Sr_2CrReO_6 (SCRO), possessing the highest Curie temperature, T_C = 635 K, among the double perovskite family [36]. For ordered SCRO, a low-temperature spin polarization of 0.86 was derived from density-

functional calculations [37], but TMR data are still not available so far. Additionally, its saturation magnetization is about only a quarter of that of SFMO [36,38]. Note that here we neglect the barrier material dependence of the parameter g_P because of the high scatter of experimental data (cf. in [31]). When comparing LSMO/$SrTiO_3$ and LSMO/$LaAlO_3$ [31], this approach results in an uncertainty of the g_P value within a factor of four. Since the bonding with oxygen does not quench the surface magnetism of the ferromagnet [39], g_P is mainly defined by the bonds of the ferromagnet with the cations of the barrier layer. Here, especially *d*-bonding to transition metal cation changes in the electronic properties at the ferromagnet/barrier layer interface. Thus, in a very crude first approximation, the parameter g_P might be scaled with the electronegativity—a measure of the ability to attract electrons—of the transition metal cations in the barrier layer. In this case, the g_P values of LSMO/$SrTiO_3$ and LSMO/TiO_2 should be nearly the same, as obtained experimentally [31]. On the other hand, the available data are too sparse to carry out such an analysis for a sufficient number of materials. Additionally, comprehensive theoretical work on this problem is still missing.

Table 1. Low-temperature spin polarization, Curie temperature, and Bloch's $T^{3/2}$ law coefficient of ferromagnetic metals and ferrimagnetic oxides.

Compound	P_0	T_C, K	g, $T^{-3/2}$
Fe	0.44 [40]	1043	2.969×10^{-5}
Co	0.34 [40]	1400	1.909×10^{-5}
LSMO	0.85 [41]	~300 [1]	1.925×10^{-4}
SFMO	0.72 [2] [34]	420	1.162×10^{-4}
SCRO	0.69 [2] [37]	635	6.249×10^{-5}
Fe_3O_4	0.55 [42]	858	3.379×10^{-5}

[1] T_C estimated for $P \to 0$ using data [31]. [2] ASD = 0.1.

Figure 1 shows the temperature dependence of the tunneling spin polarization for:

- FM metals, compared with the experimental data of CoFe/Al_2O_3/Co [8], CoFeB/Al_2O_3/CoFeB, and CoFeB/MgO/CoFeB MTJs [33];
- LSMO, compared with the experimental data of LSMO/$SrTiO_3$/LSMO [43–45], LSMO/$SrTiO_3$/LSMO, LSMO/TiO_2/LSMO, LSMO/$LaAlO_3$/LSMO [31], LSMO/$SrTiO_3$/LSMO, and LSMO/$CaTiO_3$/LSMO [46];
- SFMO, compared with the experimental data of SFMO/$SrTiO_3$/Co [41], SFMO/$SrTiO_3$/SFMO [47], and magnetite (Fe_3O_4), with the experimental data of Fe_3O_4/AlO_x/Co, Fe_3O_4/AlO_x/Ni [16], Fe_3O_4(110)/AlO_x/CoFe [48], Fe_3O_4(110)/Al_2O_3/Co [49], and Fe_3O_4/ MgO/Fe [50].

Lines are calculations, and symbols are values derived from experimental data. Note that we also have considered magnetite, which is an electric conductor at room temperature with exponentially increasing resistivity toward lower temperatures [51]. Additionally, Figure 1 nicely illustrates the strong dependence on the interface conditions discussed above.

Figure 2 depicts the TMR calculated using Equation (7), considering the temperature dependencies of tunneling spin polarization presented in Table 1 and Figure 1. The TMR in the MTJs deteriorates due to the temperature dependence of the spin polarization the lower the Curie temperature is.

As a result, MTJs consisting of FM oxides with a T_C not far above room temperature are not promising for room temperature applications. Note that we have not taken into account spin-independent tunneling that—according to Equation (8)—further reduces the TMR. Due to this reason, the experimental data of SFMO and Fe_3O_4 are lower than the calculated ones. In the case of SFMO, the value of the coefficient β_{SI} (298 K) amounts to about 0.1 [35]. On the other hand, the discovery of the coherent tunneling effect at Fe(100)/MgO(100) boundaries enables theoretically MR values of up to 1000% [9–12]. This

has shifted the research activities in the last years to MTJs employing magnetic electrodes of Fe-containing alloys. That separate effect will not be not accounted in this work.

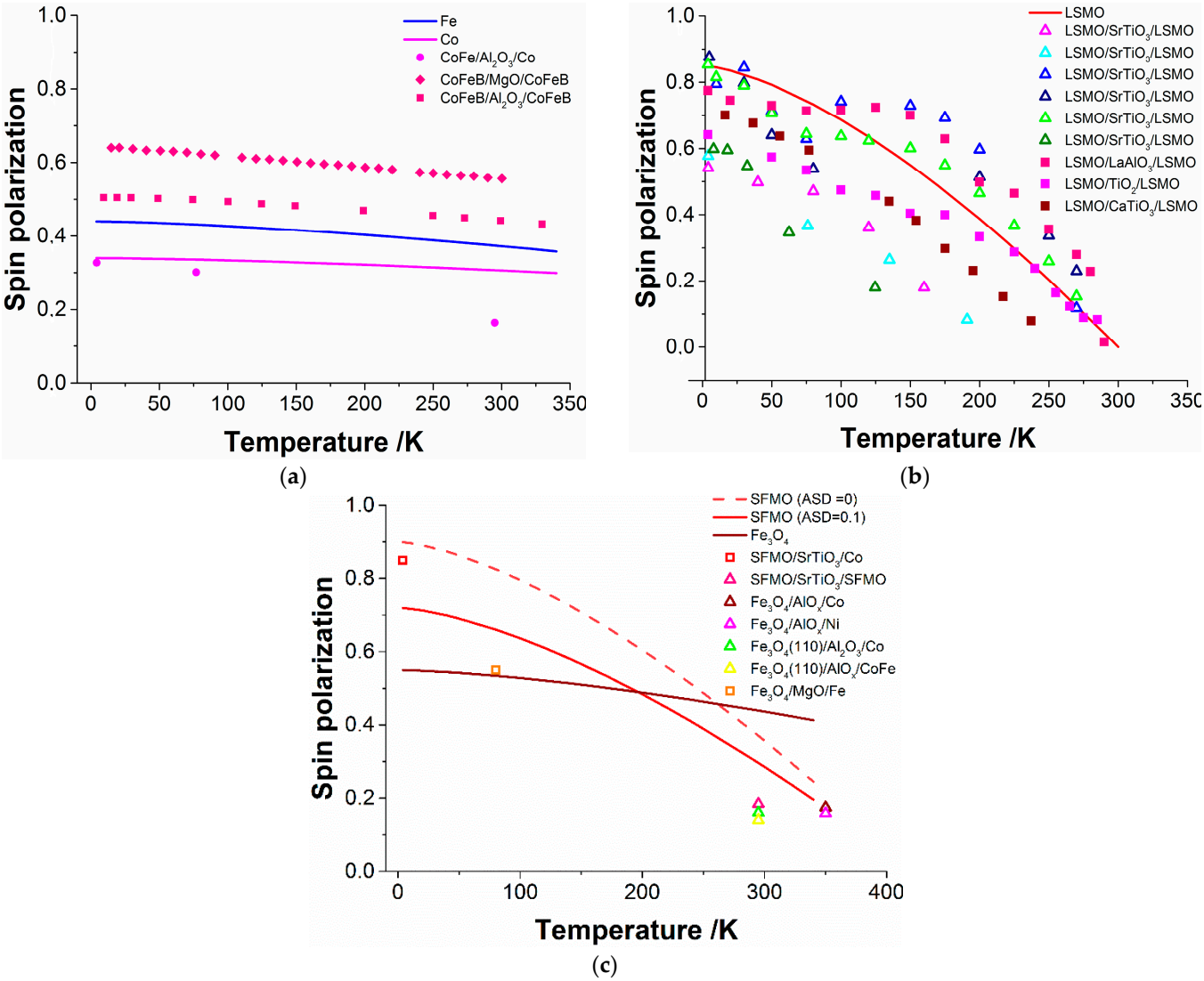

Figure 1. Temperature dependence of the tunneling spin polarization for FM metal, in comparison with experimental data of $CoFe/Al_2O_3/Co$ [8], $CoFeB/Al_2O_3/CoFeB$, and $CoFeB/MgO/CoFeB$ [33] (**a**); for LSMO, in comparison with the experimental data of $LSMO/SrTiO_3/LSMO$ [43–45], $LSMO/SrTiO_3/LSMO$, $LSMO/TiO_2/LSMO$, $LSMO/LaAlO_3/LSMO$ [31], $LSMO/SrTiO_3/LSMO$, and $LSMO/CaTiO_3/LSMO$ [46] (**b**); for SFMO, in comparison with the experimental data of $SFMO/SrTiO_3/Co$ [41] and $SFMO/SrTiO_3/SFMO$ [47], as well as Fe_3O_4 in comparison with experimental data of $Fe_3O_4/AlO_x/Co$, $Fe_3O_4/AlO_x/Ni$ [16], $Fe_3O_4(110)/AlO_x/CoFe$ [48], $Fe_3O_4(110)/Al_2O_3/Co$ [49], and $Fe_3O_4/MgO/Fe$ [50] (**c**).

In the ideal case described by Equation (7), the temperature coefficient of TMR is given by:

$$TC_{TMR} = \frac{1}{TMR}\frac{d(TMR)}{dT} = \frac{-3g_P T^{1/2}}{P_0^2(1-g_P T^{3/2})^2 - P_0^4(1-g_P T^{3/2})^4}. \quad (10)$$

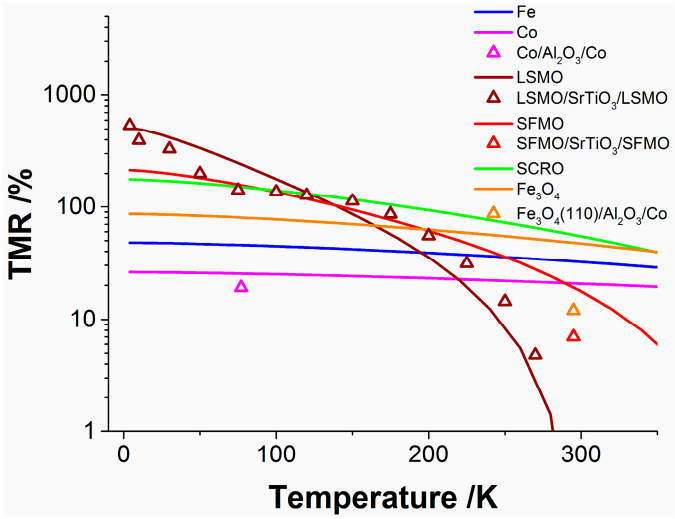

Figure 2. Temperature dependence of the TMR calculated using Equation (7), in comparison with experimental data of $Co/Al_2O_3/Ni_{80}Fe_{20}$ [52], $LSMO/SrTiO_3/LSMO$ [31], $SFMO/SrTiO_3/SFMO$ [47], and $Fe_3O_4(110)/Al_2O_3/Co$ [49].

Figure 3 shows the temperature dependence of the temperature coefficient of the TMR calculated by means of Equation (10). The value of TC_{TMR} at a given temperature depends strongly on the value of g_P and, thus, on the Curie temperature. As a result, FM materials possessing a T_C value below 650 K are not suitable for room temperature application because of an unacceptable temperature coefficient of $TC_{TMR} > -2\%$.

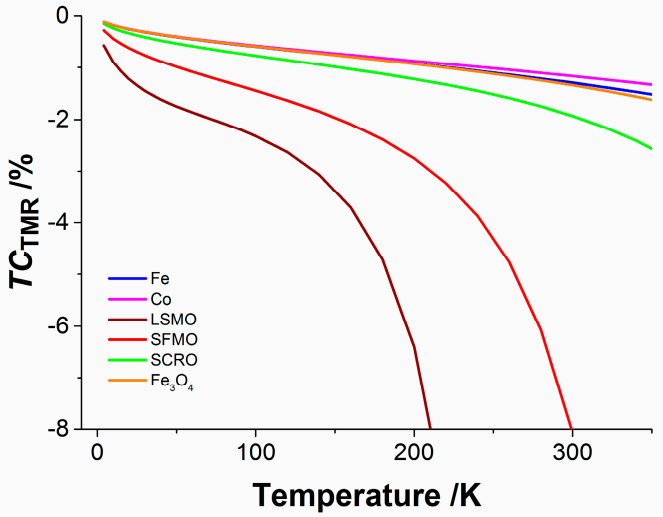

Figure 3. Temperature dependence of the temperature coefficient TC_{TMR} of the TMR calculated by means of Equation (10).

4. Conclusions

The temperature and disorder dependencies of the spin polarization were evaluated. Both the temperature dependence of the TMR and, for the very first time, its temperature coefficient were calculated based on the simplified Julliére model. The TMR in MTJs deteriorates due to the temperature dependence of the spin polarization the lower the Curie temperature is. As a result, MTJs consisting of ferromagnetic oxides with a T_C value not far above room temperature are not promising for room temperature application. Additionally, ferrimagnetic oxides possessing a Curie temperature value $T_C < 650$ K are not suitable for room temperature application because of an unacceptable temperature coefficient exceeding -2%.

Funding: This research was funded by the European Union within the scope of the European project H2020-MSCA-RISE-2017-778308–SPINMULTIFILM.

Data Availability Statement: The original contributions presented in the study are included in the article; further inquiries can be directed to the author.

Acknowledgments: The authors thank Evgenii Artiukh for his help in preparing the manuscript.

Conflicts of Interest: The authors declare no conflict of interest.

References

1. Baibich, M.N.; Broto, J.M.; Fert, A.; Nguyen Van Dau, F.; Petroff, F.; Etienne, P.; Creuzet, G.; Friederich, A.; Chazelas, J. Giant magnetoresistance of (001)Fe/(001) Cr magnetic superlattices. *Phys. Rev. Lett.* **1988**, *61*, 2472–2475. [CrossRef] [PubMed]
2. Binasch, G.; Grünberg, P.; Saurenbach, F.; Zinn, W. Enhanced magnetoresistance in layered magnetic structures with antiferromagnetic interlayer exchange. *Phys. Rev. B* **1989**, *39*, 4828–4830. [CrossRef]
3. Peng, S.; Zhang, Y.; Wang, M.; Zhang, Y.; Zhao, W. *Magnetic Tunnel Junctions for Spintronics: Principles and Applications*; Wiley: Hoboken, NJ, USA, 2014; pp. 1–16.
4. Dieny, B.; Prejbeanu, I.L.; Garello, K.; Gambardella, P.; Freitas, P.; Lehndorff, R.; Raberg, W.; Ebels, U.; Demokritov, S.O.; Akerman, J.; et al. Opportunities and challenges for spintronics in the microelectronic industry. *Nat. Electron.* **2020**, *3*, 446–459. [CrossRef]
5. Tedrow, P.M.; Meservey, R. Spin-dependent tunneling into ferromagnetic nickel. *Phys. Rev. Lett.* **1971**, *26*, 192–195. [CrossRef]
6. Julliere, M. Tunnelling between FM films. *Phys. Lett. A* **1975**, *54*, 225–226. [CrossRef]
7. Miyazaki, T.; Tezuka, N. Giant magnetic tunneling effect in Fe/Al_2O_3/Fe junction. *J. Magn. Magn. Mater.* **1995**, *139*, L231–L234. [CrossRef]
8. Moodera, J.S.; Kinder, L.R.; Wong, T.M.; Meservey, R. Large magnetoresistance at room temperature in ferromagnetic thin film tunnel junctions. *Phys. Rev. Lett.* **1995**, *74*, 3273–3276.
9. Butler, W.H.; Zhang, X.-G.; Schulthess, T.C.; MacLaren, J.M. Spin-dependent tunneling conductance of Fe | MgO | Fe sandwiches. *Phys. Rev. B* **2001**, *63*, 054416. [CrossRef]
10. Mathon, J.; Umerski, A. Theory of tunneling magnetoresistance of an epitaxial Fe/MgO/Fe(001) junction. *Phys. Rev. B* **2001**, *63*, 220403. [CrossRef]
11. Parkin, S.P.; Kaiser, C.; Panchula, A.; Rice, P.M.; Hughes, B.; Samant, M.; Yang, S.H. Giant tunnelling magnetoresistance at room temperature with MgO(100) tunnel barriers. *Nat. Mater.* **2004**, *3*, 862–867. [CrossRef]
12. Yuasa, S.; Nagahama, T.; Fukushima, A.; Suzuki, Y.; Ando, K. Giant roomtemperature magnetoresistance in single-crystal Fe/MgO/Fe magnetic tunnel junctions. *Nat. Mater.* **2004**, *3*, 868–871. [CrossRef] [PubMed]
13. Bibes, M.; Barthélémy, A. Oxide Spintronics. *IEEE Trans. Electron. Dev.* **2007**, *54*, 1003–1023. [CrossRef]
14. Slonczewski, J. Conductance and exchange coupling of two ferromagnets separated by a tunneling barrier. *Phys. Rev. B* **1989**, *39*, 6995–7002. [CrossRef]
15. MacLaren, J.M.; Zhang, X.-G.; Butler, W.H. Validity of the Julliere model of spin-dependent tunneling. *Phys. Rev. B* **1997**, *56*, 11827–11832. [CrossRef]
16. Opel, M.; Geprägs, S.; Menzel, E.P.; Nielsen, A.; Reisinger, D.; Nielsen, K.-W.; Brandlmaier, A.; Czeschka, F.D.; Althammer, M.; Weiler, M.; et al. Novel multifunctional materials based on oxide thin films and artificial heteroepitaxial multilayers. *Phys. Status Solidi A* **2011**, *208*, 232–251. [CrossRef]
17. De Teresa, J.M.; Barthélémy, A.; Fert, A.; Contour, J.P.; Montaigne, F.; Seneor, P. Role of metal-oxide interface in determining the spin polarization of magnetic tunnel junctions. *Science* **1999**, *286*, 507–509. [CrossRef] [PubMed]
18. Zhang, S.; Levy, P.M. Models for magnetoresistance in tunnel junctions. *Eur. Phys. J. B* **1999**, *10*, 599–606. [CrossRef]
19. Tsymbal, E.Y.; Pettifor, D.G. The influence of impurities within the barrier on tunneling magnetoresistance. *J. Appl. Phys.* **1999**, *85*, 5801–5803. [CrossRef]
20. Kobayashi, K.I.; Kimura, T.; Sawada, H.; Terakura, K.; Tokura, Y. Room-temperature magnetoresistance in an oxide material with an ordered double-perovskite structure. *Nature* **1998**, *395*, 677–680. [CrossRef]
21. Gadzuk, J.W. Band-structure effects in the field-induced tunneling of electrons from metals. *Phys. Rev.* **1969**, *182*, 416–426.
22. Mazin, I.I. How to define and calculate the degree of spin polarization in ferromagnets. *Phys. Rev. Lett.* **1999**, *83*, 1427–1430. [CrossRef]
23. Soulen, R.J., Jr.; Byers, J.M.; Osofsky, M.S.; Nadgorny, B.; Ambrose, T.; Cheng, S.F.; Broussard, P.R.; Tanaka, C.T.; Nowak, J.; Moodera, J.S.; et al. Measuring the spin polarization of a metal with a superconducting point contact. *Science* **1998**, *282*, 85–88. [PubMed]
24. Feder, R.; Pleyer, H. On the feasibility of studying surface magnetism by spin-polarized low-energy electron diffraction. *Surf. Sci.* **1982**, *117*, 285–293. [CrossRef]
25. Shang, C.H.; Nowak, J.; Jansen, R.; Moodera, J.S. Temperature dependence of magnetoresistance and surface magnetization in ferromagnetic tunnel junctions. *Phys. Rev. B* **1998**, *58*, R2917–R2920. [CrossRef]
26. Meservy, R.; Tedrow, P.M. Spin polarized electron tunneling. *Phys. Rep.* **1994**, *238*, 173–243. [CrossRef]

27. Pierce, D.T.; Celotta, R.J.; Unguris, J.; Siegmann, H. Spin-dependent elastic scattering of electrons from a ferromagnetic glass. $Ni_{40}Fe_{40}B_{20}$. *Phys. Rev. B* **1982**, *26*, 2566–2574. [CrossRef]
28. MacDonald, A.H.; Jungwirth, T.; Kasner, M. Temperature dependence of itinerant electron junction magnetoresistance. *Phys. Rev. Lett.* **1998**, *81*, 705–708. [CrossRef]
29. Mauri, D.; Scholl, D.; Siegmann, H.C.; Kay, E. Observation of the exchange interaction at the surface of a ferromagnet. *Phys. Rev. Lett.* **1988**, *61*, 758–761. [CrossRef]
30. Mills, D.L.; Maradudin, A.A. Some thermodynamic properties of a semi-infinite Heisenberg ferromagnet. *J. Phys. Chem. Solids* **1967**, *28*, 1855–1874. [CrossRef]
31. Garcia, V.; Bibes, M.; Barthélémy, A.; Bowen, M.; Jacquet, E.; Contour, J.-P.; Fert, A. Temperature dependence of the interfacial spin polarization of $La_{2/3}Sr_{1/3}MnO_3$. *Phys. Rev. B* **2004**, *69*, 052403. [CrossRef]
32. Balcells, L.; Navarro, J.; Bibes, M.; Roig, A.; Martínez, B.; Fontcuberta, J. Cationic ordering control of magnetization in Sr_2FeMoO_6 double perovskite. *Appl. Phys. Lett.* **2001**, *78*, 781–783. [CrossRef]
33. Kou, X.; Schmalhorst, J.; Thomas, A.; Reiss, G. Temperature dependence of the resistance of magnetic tunnel junctions with MgO barrier. *Appl. Phys. Lett.* **2006**, *88*, 212115. [CrossRef]
34. Artsiukh, E.; Suchaneck, G. Intergranular magnetoresistance of strontium ferromolybdate ceramics caused by spin-polarized tunneling. *Open Ceram.* **2021**, *7*, 100171. [CrossRef]
35. Suchaneck, G.; Artiukh, E.; Sobolev, N.A.; Telesh, E.; Kalanda, N.; Kiselev, D.A.; Ilina, T.S.; Gerlach, G. Strontium ferromolybdate-based magnetic tunnel junctions. *Appl. Sci.* **2022**, *12*, 2717. [CrossRef]
36. Kato, H.; Okuda, T.; Okimoto, Y.; Tomioka, Y.; Takenoya, Y.; Ohkubo, A.; Kawasaki, M.; Tokura, Y. Metallic ordered double-perovskite Sr_2CrReO_6 with maximal Curie temperature of 635 K. *Appl. Phys. Lett.* **2002**, *81*, 328–330. [CrossRef]
37. Vaitheeswaran, G.; Kanchana, V.; Delin, A. Pseudo-half-metallicity in the double perovskite Sr_2CrReO_6 from density-functional calculations. *Appl. Phys. Lett.* **2005**, *86*, 032513. [CrossRef]
38. Geprägs, S.; Czeschka, F.D.; Opel, M.; Goennenwein, S.T.B.; Yu, W.; Mader, W.; Gross, R. Epitaxial growth and magnetic properties of Sr_2CrReO_6 thin films. *J. Magn. Magn. Mater.* **2009**, *321*, 2001–2004. [CrossRef]
39. Tsymbal, E.Y.; Oleinik, I.I.; Pettifor, D.G. Oxygen-induced positive spin polarization from Fe into the vacuum barrier. *J. Appl. Phys.* **2000**, *87*, 5230–5232. [CrossRef]
40. Tedrow, P.M.; Meservey, R. Spin polarization of electrons tunneling from films of Fe, Co, Ni, and Gd. *Phys. Rev. B* **1973**, *7*, 318–326. [CrossRef]
41. Bibes, M.; Bouzehouane, K.; Barthélémy, A.; Besse, M.; Fusil, S.; Bowen, M.; Seneor, P.; Carrey, J.; Cros, V.; Vaurès, A.; et al. Tunnel magnetoresistance in nanojunctions based on Sr_2FeMoO_6. *Appl. Phys. Lett.* **2003**, *83*, 2629–2631. [CrossRef]
42. Alvarado, S.F.; Erbudak, M.; Munz, P. Final-state effects in the 3d photoelectron spectrum of Fe_3O_4 and comparison with Fe_xO. *Phys. Rev. B* **1976**, *14*, 2740–2745. [CrossRef]
43. Sun, J.Z.; Gallagher, W.J.; Duncombe, P.R.; Krusin-Elbaum, L.; Altman, R.A.; Gupta, A.; Lu, Y.; Gong, G.Q.; Xiao, G. Observation of large low-field magnetoresistance in trilayer perpendicular transport devices made using doped manganate perovskites. *Appl. Phys. Lett.* **1996**, *69*, 3266–3268. [CrossRef]
44. Li, X.W.; Lu, Y.; Gong, G.Q.; Xiao, G.; Gupta, A.; Lecoeur, P.; Sun, J.Z.; Wang, Y.Y.; Dravid, V.P. Epitaxial $La_{0.67}Sr_{0.33}MnO_3$ magnetic tunnel junctions. *J. Appl. Phys.* **1997**, *81*, 5509–5511. [CrossRef]
45. Bowen, M.; Bibes, M.; Barthélémy, A.; Contour, J.-P.; Anane, A.; Lemaître, Y.; Fert, A. Nearly total spin polarization in $La_{2/3}Sr_{1/3}MnO_3$ from tunneling experiments. *Appl. Phys. Lett.* **2003**, *82*, 233–235. [CrossRef]
46. O'Donnell, J.; Andrus, A.E.; Oh, S.; Colla, E.V.; Eckstein, J.N. Colossal magnetoresistance magnetic tunnel junctions grown by molecular-beam epitaxy. *Appl. Phys. Lett.* **2000**, *76*, 1914–1916. [CrossRef]
47. Kumar, N.; Misra, P.; Kotnala, R.K.; Gaur, A.; Katiyar, R.S. Room temperature magnetoresistance in $Sr_2FeMoO_6/SrTiO_3/Sr_2FeMoO_6$ trilayer devices. *J. Phys. D Appl. Phys.* **2014**, *47*, 065006. [CrossRef]
48. Matsuda, H.; Takeuchi, M.; Adachi, H.; Hiramoto, M.; Matsukawa, N.; Odagawa, A.; Setsune, K.; Sakakima, H. Fabrication and magnetoresistance properties of spin-dependent tunnel junctions using an epitaxial Fe_3O_4 film. *Jpn. J. Appl. Phys.* **2002**, *41*, L387–L390. [CrossRef]
49. Nagahama, T.; Matsuda, Y.; Tate, K.; Kawai, T.; Takahashi, N.; Hiratani, S.; Watanabe, Y.; Yanase, T.; Shimada, T. Magnetic properties of epitaxial Fe_3O_4 films with various crystal orientations and tunnel magnetoresistance effect at room temperature. *Appl. Phys. Lett.* **2014**, *105*, 102410. [CrossRef]
50. Yasui, S.; Honda, S.; Okabayashi, J.; Yanase, T.; Shimada, T.; Nagahama, T. Large inverse tunnel magnetoresistance in magnetic tunnel junctions with an Fe_3O_4 electrode. *Phys. Rev. Appl.* **2021**, *15*, 034042. [CrossRef]
51. Takahashi, N.; Huminiuc, T.; Yamamoto, Y.; Yanase, T.; Shimada, T.; Hirohata, A.; Nagahama, T. Fabrication of epitaxial Fe_3O_4 film on a Si(111) substrate. *Sci. Rep.* **2017**, *7*, 7009. [CrossRef]
52. Jansen, A.R.; Moodera, J.S. Enhanced tunnel magnetoresistance in Fe-doped Al_2O_3 barriers. *Appl. Phys. Lett.* **1999**, *75*, 400–402. [CrossRef]